

Supersonic Random Flows in the Perseus Molecular Cloud

Paolo Padoan

Theoretical Astrophysics Center, Juliane Maries Vej 30, DK-2100 Copenhagen, Denmark

John Bally & Youssef Billawala

*Department of Astrophysics, Planetary, and Atmospheric Sciences,
Center for Astrophysics and Space Astronomy,
Campus Box 389, University of Colorado, Boulder CO 80309*

Mika Juvela

Helsinki University Observatory, Tähtitorninmäki, P.O.Box 14, SF-00014 University of Helsinki, Finland

Åke Nordlund

*Astronomical Observatory and Theoretical Astrophysics Center,
Juliane Maries Vej 30, DK-2100 Copenhagen, Denmark*

ABSTRACT

We compare the statistical properties of $J=1\rightarrow 0$ ^{13}CO spectra observed in the Perseus Molecular Cloud with synthetic $J=1\rightarrow 0$ ^{13}CO spectra from a 5 pc model cloud. The synthetic spectra are computed solving the non-LTE radiative transfer problem for a model cloud obtained as solutions of the 3-D magneto-hydrodynamic (MHD) equations in both the highly supersonic and super-Alfvénic regimes of random flows.

We present several statistical results that demonstrate remarkable similarity between real data and the synthetic cloud. The three-dimensional structure and dynamics of molecular clouds like Perseus are appropriately described by random supersonic and super-Alfvénic MHD flows. Although the description of gravity and stellar radiation are essential to understand the formation of single protostars and the effects of star formation in the cloud dynamics, the overall description of the cloud and of the initial conditions for star formation can apparently be described on intermediate scales without accounting for gravity and stellar radiation.

Subject headings: turbulence – ISM: kinematics and dynamics – magnetic fields – individual (Perseus Cloud); radio astronomy: interstellar: lines

arXiv:astro-ph/9711008v1 3 Nov 1997

1. Introduction

The structure and dynamics of molecular clouds (MCs) has been the subject of intensive investigation during the past two decades. Since MCs are the sites of star formation, their properties provide insights into the initial conditions needed to form stars. On the other hand, energy injected into the clouds by young stars is also believed to play a crucial role in the cloud dynamics and evolution (e.g. Whitworth 1979; Bally & Lada 1983; Miesch & Bally 1994). The observed state of a cloud represents the balance between energy injection and dissipation.

Observations show that cloud internal motions are highly supersonic, incoherent, and random (e.g. Bally et al. 1987, 1989, 1990). Furthermore, the cloud structure is complex and by many measures is suggestive of the presence of random flows. Indeed, many authors have attempted to describe clouds using various models of turbulence (e.g. Ferrini, Marchesoni & Vulpiani 1983; Henriksen & Turner 1984; Scalo 1987; Fleck 1988; Fleck 1996) inspired by the scaling laws observed in the interstellar medium (Larson 1981). More recently, there have been several attempts to describe cloud morphology and velocity fields using fractals (e.g. Scalo 1990; Falgarone & Phillips 1991; Falgarone, Phillips & Walker 1991; Falgarone 1992; Larson 1995; Elmegreen 1997).

Most theoreticians have argued that clouds are supported by magnetic fields (Mestel 1965; Strittmatter 1966; Parker 1973; Mouschovias 1976a, b; McKee & Zweibel 1995) and interpreted the observed line-widths in terms of magneto-hydrodynamic (MHD) waves (Arons & Max 1975; Zweibel & Josafatsson 1983; Elmegreen 1985, Falgarone & Puget 1986). However, comparison of the extinction statistics with recent models of supersonic and super-Alfvénic random flows suggests that such models may provide a superior description of MCs (Padoan, Jones & Nordlund 1997). OH Zeeman measurements (Crutcher et al. 1993; Crutcher et al. 1996) have also been shown to be consistent with the predictions of a super-Alfvénic random flow (Padoan & Nordlund 1997).

In this paper, we compare some observed properties of the Perseus molecular cloud with the predictions of supersonic and super-Alfvénic random flows. We start with a self-consistent MHD simulation of a random flow in a 3-D 128^3 grid (Padoan & Nordlund 1997). We solve the radiative transfer problem using a non-LTE Monte Carlo approach (Juvela 1997) to

compute ^{13}CO synthetic spectra on a 90 by 90 cell grid with 60 velocity channels. Remarkable agreement of these models with the data is illustrated by several results. These results demonstrate that such models provide an excellent description for the kinematics and structure of molecular clouds despite the absence of gravity, external radiation fields, or stellar outflows in the models.

2. The Perseus Molecular Cloud

Observations of the Perseus molecular cloud complex were made from 1985 to 1991 with AT&T Bell Laboratories 7 m offset Cassegrain antenna in Holmdel, New Jersey. Approximately a 6° by 4° region was surveyed in the 110 GHz line of $J=1\rightarrow 0$ ^{13}CO . The observations were made on a $1'$ grid with a $100''$ beam yielding 33,000 spectra, each with 128×100 kHz channels (0.273 km s^{-1}). See Billawala et al. (1997) for further details of observations and discussion of the cloud structure.

The Perseus molecular cloud is roughly a 6° by 2° region located at a distance estimated to range from 200 to 350 pc (Herbig & Jones 1983; Cérnis 1990) and has a projected size of 30 by 10 pc (see figure 1). The cloud is part of the larger Taurus-Auriga-Perseus complex and lies below the galactic plane ($b \sim -20^\circ$) with an estimated mass of $10^4 M_\odot$ (Billawala et al. 1997).

The complex has produced some high mass stars at its eastern end which lie near the centroid of Perseus OB2 association, a loose grouping of 5 to 10 O and B stars, that is about 7 million years old (Blaauw 1991). Perseus OB2 has blown a 20° diameter (100 pc) supershell into the surrounding interstellar medium that can be seen in 21 cm H I data (Heiles 1984). The shell is partially superimposed on the Perseus molecular cloud and may be interacting with it. Perseus contains two young stellar clusters and a background of relatively inactive molecular gas that has formed few stars.

Near the eastern end is the young (< 7 Myr old) cluster IC348, which has several hundred members and may still be forming (Strom, Grasdalen & Strom 1974; Lada, Strom & Myers 1993; Lada & Lada 1995). Omicron Persei, a B1 III star, located near the center, is believed to be a few parsecs in front of the cloud (Bachiller et al. 1987). Lada & Lada (1995) estimate a cluster population of ≈ 380 stars with a highly centralized distribution falling off inversely

with distance from the inner 0.1 pc diameter core which contains about $\sim 200 M_{\odot}$ of stars and a density of $220 M_{\odot} \text{ pc}^{-3}$. Star formation has been going on for at least 5 to 7 Myr at a roughly constant rate and with an efficiency of $\sim 50\%$.

A second and even younger cluster is embedded in the Perseus cloud several degrees to the west near the reflection nebula NGC1333. This region contains the most active site of ongoing star formation in Perseus. NGC1333 contains an embedded < 1 Myr old infrared cluster, a large number of molecular outflows (Knee & Sandell 1997), Herbig–Haro objects (Bally, Devine & Reipurth 1996), and shock excited near-infrared H_2 emission regions (Aspin, Sandell & Russell 1994; Hodapp & Ladd 1995; Sandell et al. 1994). Lada, Alves & Lada (1996) find 143 young stars in a 432 square arc-minute region with most being members of two prominent sub-clusters. More than half of these stars display infrared excess emission, a signature of young stellar objects. Lada et al. estimate the age of the cluster to be less than 10^6 years with a star formation rate of $4 \times 10^{-5} M_{\odot} \text{ yr}^{-1}$.

Away from IC348 and NGC1333, the Perseus cloud contains about a dozen dense cloud cores with low levels of star formation activity including the dark cloud B5 (Langer 1989; Bally, Devine, & Alten 1996) at its eastern end, the cold core B1 for which a magnetic field has been measured by means of OH Zeeman (Goodman et al. 1989; Crutcher et al. 1993), and the dark clouds L1448 and L1455 on the west end (Bally et al. 1997).

The cloud exhibits a wealth of sub-structures such as cores, shells, and filaments and dynamical structures including stellar outflows and jets, and a large scale velocity gradient. While emission at the western end of the complex lies mostly near $v_{lsr} = 4 \text{ km s}^{-1}$ (L1448), the eastern end of the complex has a velocity of $v_{lsr} = 10.5 \text{ km s}^{-1}$ (B5). This may be an indication that we are seeing several smaller clouds partially superimposed along the line of sight (C ernis 1990).

3. Theoretical Models

Padoan et al. (1997) computed synthetic molecular clouds containing grids of 90×90 spectra of different molecular transitions for a total of more than a half a million spectra. The spectra were obtained with a non-LTE Monte Carlo code (Juvela 1997) starting from density and velocity fields that provide realistic descriptions of the observed physical condi-

tions in MCs. The density and velocity fields are obtained as solutions of the magneto-hydrodynamic (MHD) equations in a 128^3 grid and in both super-Alfv enic and highly supersonic regimes of random flows (Padoan & Nordlund 1997). The resulting density fields span a continuous range of values from 0.1 to 10^5 cm^{-3} which produce column densities ranging over three orders of magnitude or more. These cloud models have already been shown to reproduce observed statistical properties of MCs (Padoan, Jones & Nordlund 1997; Padoan & Nordlund 1997).

In this work we use a 90×90 grid of spectra of $\text{J}=1 \rightarrow 0$ ^{13}CO from a 5 pc diameter artificial cloud. For a detailed description of the construction of the synthetic spectra we refer the reader to Padoan et al. (1997).

The MHD numerical experiment which produces the synthetic cloud does not account for gravity, stellar radiation, or stellar outflows. However, the numerical flow is consistent with the general observed properties of dark clouds such as the existence of random and supersonic motions. The mean density and rms velocity in the model are related to the physical size of the computational grid via Larson’s interstellar medium scaling laws (Larson 1981). A 5 pc model has been selected because the Perseus complex looks like a string of smaller clouds with an estimated size of a few parsecs. The mean density of the 5 pc model is $400 \text{ H}_2 \text{ molecules cm}^{-3}$. This corresponds to a total mass of $3.2 \times 10^3 M_{\odot}$ (using a mean molecular weight of $\mu = 2.6$ to correct for He).

4. Statistics of the Observed and Synthetic Spectra

Figure 1 shows the integrated $\text{J}=1 \rightarrow 0$ ^{13}CO map of the Perseus complex. The two brightest emission regions lie near the young stellar clusters IC348 (left) and NGC1333 (right). Complex and filamentary structure is evident in this image, in the individual channel maps, and in images of peak antenna temperature (Billawala et al. 1997). Figure 2 left and center panels show close-up views of the L1448 and B5 dark clouds respectively. Figure 2 on the right shows one particular synthetic map used in our analysis. It is obtained from the 5 pc cloud model and shows the integrated antenna temperature of the $\text{J}=1 \rightarrow 0$ ^{13}CO synthetic spectra as the three observed maps in figures 1 and 2. As the real data, the synthetic image shows filamentary structure, cores, and

partial shells.

Fig. 3 shows the mean spectrum obtained by averaging all spectra lying within the boundaries of the maps of each of three regions; B5, L1448, and the entire Perseus complex. We over-plot the synthetic mean spectrum computed from the 5 pc synthetic map (dashed lines). The spectra are centered about their own mean. The high velocity blue-shifted tail in the L1448 spectrum may be produced by an unrelated cloud superimposed along the line-of-sight. The B5 cloud has been estimated to have a mass of slightly less than $10^3 M_{\odot}$ (Langer et al. 1989) while the mass of L1448 has been estimated to be about $500 M_{\odot}$ by Bally et al. (1997). These results are consistent with the narrower width of the mean spectra as compared to the width of the mean spectrum of the more massive ($3200 M_{\odot}$) theoretical model. The mean spectrum of the entire Perseus cloud is wider than that of the theoretical model for different reasons. First, the total mass of the Perseus complex is about $10^4 M_{\odot}$ (Billawala et al. 1997). Second, there is a large scale systematic velocity gradient from the eastern to the western ends of the complex which are not taken into account in our models. The projected length of the cloud is 30 pc, far larger than the size of our model. Finally, there is evidence that this gradient is produced by the superposition of two clouds that may be as far as 100 pc distant from each other (C ernis 1990; Herbig & Jones 1983).

The probability distributions of the velocity integrated antenna temperature for L1448, B5, and the entire Perseus cloud are plotted in Fig. 4. The theoretical result derived from the 5 pc diameter model cloud is over-plotted in dashed lines. Though there are individual differences between the clouds and the model, the overall shapes of the distributions are qualitatively similar in that they are dominated by intermittent tails. Differences between L1448 and B5 may be in part due to line-of-sight confusion and small number statistics. For the entire Perseus cloud, the main difference may be attributable to the fact that it is a much larger cloud than our model. The distributions of larger models are in fact expected to be more intermittent (Padoan & Nordlund 1997). Since the integrated antenna temperature is proportional to the column density, this result shows that the theoretical density distribution is consistent with the observed one.

Figure 5, 6, and 7 show 30 by 30 grids (30' by 30' for the real data) of spectra for L1448, B5, and

the model respectively. In all three figures, we have selected the highest intensity regions of these three maps. Note the qualitative similarity between the real data and the model spectra.

Figure 8 through 11 show histograms of the first four statistical moments of the individual spectra for all of Perseus, L1448, B5, and the model respectively. The plots in the upper left show the distributions of velocity centroids centered around their means. The upper right plots show the distributions of the line velocity dispersions (the line widths). The lower left plots show the skewness of these profiles which measures the degree of asymmetry present in the profiles. The observed histograms, like the theoretical ones, present a distribution of skewness values around 0, that is the gaussian value. They have a bit more extended tails than the theoretical histograms, but unfortunately the tails are rather sensitive to the noise in the observed spectra, and there is no general way to deal with the noise in order to make the tails statistically significant. The lower right plots show the kurtosis which measures the intermittency (high velocity tails) in the spectra. The distribution of kurtosis for the theoretical cloud are similar to the observed distributions. However, the observed peaks are centered around 2.3 rather than 3.0 for the theoretical model. The vertical dashed lines correspond to the values of the same statistical moments in the mean spectra shown in figure 3.

Scatter plots of the equivalent width versus velocity integrated antenna temperature are shown in Fig. 12. The equivalent width is here defined as the velocity integrated antenna temperature divided by the peak antenna temperature in each spectrum. Note that the theoretical and real data agree in magnitude, in dispersion, and have a similar overall shapes. The observed values of the line-width at the lowest integrated temperatures are a bit smaller than the theoretical ones, but that region of the plots should not be compared with the theoretical results, because the contribution from the noise in the observed spectra is there too strong. B5 apparently has a smaller equivalent width for every value of integrated temperature probably because it is a smaller cloud and is less dynamic than L1448. Over a half-dozen active outflows have been discovered in L1448 (Bally et al. 1997) while only two are known in B5 (Bally, Devine & Alten 1996).

5. Discussion and Results

The model we constructed was built upon very general considerations and not tailored to the specific characteristics of the Perseus molecular cloud or individual cores. Only the general interstellar medium scaling laws (Larson 1981) have been used to fix the physical size of the cloud model. The model has been inspired by the observation that random supersonic motions are ubiquitous in molecular clouds.

The dynamic range of length scales covered by the MHD calculations ranges from 0.04 pc to 5 pc (128^3 grid-points). The radiative transfer calculations and the resulting spectra cover a linear scale range from 0.05 pc to 5 pc (90^3 grid-points). However, numerical dissipation effectively degrades this resolution by a factor of two to an inner scale of about 0.1 pc. Thus the inner scale of the theoretical models are comparable to the linear resolution of the $100''$ beam used in our observations. The Bell Labs 7 meter telescope beam has a linear resolution of about 0.14 pc (assuming a distance of 300 pc for the Perseus cloud) and the maximum extent of the Perseus cloud that has been mapped is about 30 pc.

Giant molecular clouds (GMCs; $M > 10^5 M_\odot$ and $L \approx 20$ to 50 pc) are gravitationally bound. This must be the case since the product of the internal velocity dispersion squared times the density is one to two orders of magnitude greater than the pressure of the surrounding interstellar medium. Gravity must provide the restoring force on the scale of a GMC, otherwise GMCs would be dispersed before they could form any stars. Individual stars form from the gravitational contraction of small cores with sizes of order 0.1 pc, while clusters of stars such as IC348 and NGC1333 form from cores about 1 pc in diameter. Thus gravity is certainly important on the very large scale of GMCs ($L > 20$ pc) and on the very small scales of dense star forming cores ($L \leq 1$ pc). Our model and observations have linear dimensions intermediate between these two scales. The results of this work show that on intermediate scales the observed properties of molecular clouds and likely the initial conditions for star formation can be appropriately described without explicitly accounting for gravity. Self-gravitating cores may occasionally condense from the random flow where a local over-density is produced statistically. However, at any one time, only a fraction of the total mass is involved in such condensations. If indeed self-gravitating cores condense from

the intermittency of the random flow, then it might be possible to predict the mass spectrum of the resulting condensations which produce stars. This may be an important ingredient in constructing the initial stellar mass function (Padoan, Nordlund & Jones 1997).

In this picture, the overall density structure inside a GMC is *not* the result of gravitational fragmentation, but rather of the presence of supersonic random motions together with the short cooling time of the molecular gas. We predict that there are several shocks in the gas along any line-of-sight with velocities comparable to the overall cloud line-width. These shocks have velocities of order 1 to 10 km s⁻¹ which are not observable in the forbidden lines in the visible portion of the spectrum. However, there are several far-infrared transitions such as the 157 μm fine-structure line of C⁺, the 63 μm line of O I, and the 28, 17, and 12 μm $v = 0-0$ lines of H₂ which are readily excited by such shocks. The COBE and ISO satellites have shown that these transitions together carry about 0.1% of the total luminosity of a typical galaxy (Wright et al. 1991; cf. Lord et al. 1996). We predict that roughly 10% of this emission is produced by the shocks discussed above because these transitions are the primary coolants in the post-shock gas.

The dissipation of the kinetic energy of internal motions, E_{GMC} , by shocks in a GMC produces a luminosity of order $L_{GMC} \approx E_{GMC}/\tau_{GMC} \approx 3 \times 10^3 (L_\odot) E_{51} \tau_{4 \times 10^6}$, where the dynamical time is taken to be a cloud crossing time, $\tau_{GMC} = R_{GMC}/\sigma_{GMC}$ and σ_{GMC} is the cloud velocity dispersion. Since the above infrared transitions are the main coolants in the post-shock layers of these low velocity shocks, we expect that future observations of clouds like Perseus will show extended bright emission in these infrared transitions.

Observations of young stellar populations show that stars form from GMCs over a period of order 10 to 20 Myrs (Blaauw 1991) which implies that clouds must survive for at least this long. Since this time-scale exceeds the dissipation time, the internal motions must be regenerated. There are several possible sources for such energy generation. When massive stars are present, their radiation, winds, and supernova explosions inject large amounts of energy into the surrounding gas. However this amount of energy is far in excess of what is required to balance the dissipation of kinetic energy in shocks. Massive stars are likely to be responsible for cloud disruption.

The second candidate energy source is outflows from low mass stars which form more uniformly throughout the cloud (Strom et al. 1989; Strom, Margulis & Strom 1989). The Perseus molecular cloud contains only intermediate to low mass stars, which during their first 10^5 years of life produced jets and outflows. All the cores studied here are known to have multiple outflows. Over a dozen outflows in NGC1333, 8 groups of Herbig–Haro objects in L1448, and 2 outflows in B5 have been discovered. Outflows can provide the mechanism to stir the clouds and balance the dissipation of the random supersonic motions.

The plots of equivalent width versus integrated antenna temperature in figure 12 support the scenario described above. While the plot for L1448 is in excellent agreement with the model, the plot for B5 shows a systematically lower equivalent width. This is consistent with the lower number of outflows discovered in B5 relative to L1448.

However, the main source of energy for the small and intermediate scale differential velocity field may simply be cascading of energy from larger scales. The dynamical times of inertial scale motions are short compared to those of the larger scale motions. In the inertial range, there is a quasi-steady flow of energy from larger scales towards the energy dissipation scales. The numerical simulations represents only piece of the inertial range, and hence, on these scales, energy input at the largest wavenumbers is to be expected.

On the largest, energy carrying scales, we have already remarked that the motions must be constrained by gravity. Gravity field fluctuations large enough to constrain these clouds must come from self-gravity, and from interactions with neighboring clouds and embedded stars. The time variations and tidal effects due to relative motions of the self-gravitating masses is perhaps the main source of energy input at the large scale end of the inertial cascade.

Padoan, Jones & Nordlund (1997) and Padoan & Nordlund (1997) have shown that the statistics of infrared stellar extinction (Lada et al. 1994) and the OH Zeeman measurements (Crutcher et al. 1993; Crutcher et al. 1996) can be explained by our model of supersonic random flows. In the present work, we have shown that the same model is consistent with molecular clouds observed in the $J=1\rightarrow 0$ ^{13}CO line. These results together provide compelling evidence that *supersonic and super-Alfvénic random flows correctly describe the structure and dynamics of molecu-*

lar clouds.

This work has been partially supported by the Danish National Research Foundation through its establishment of the Theoretical Astrophysics Center. Computing resources were provided by the Danish National Science Research Council, and by the French ‘Centre National de Calcul Parallèle en Science de la Terre’. PP is grateful to the Center for Astrophysics and Space Astronomy (CASA) in Boulder (Colorado) for the warm hospitality offered during the period in which this paper has been written. JB and YB acknowledge support from NASA grant NAGW-4590 (Origins) and NASA grant NAGW-3192 (LTSA). The work of MJ was supported by the Academy of Finland Grant No. 1011055.

REFERENCES

- Arons, J. & Max, C. E. 1975, *ApJ*, 196, L77
- Aspin, C., Sandell, G. & Russell, A. P. G. 1994, *A&AS*, 106, 165
- Bachiller, R., Cernicharo, J., Omont, A. & Goldsmith, P. 1987, *A&A*, 185, 297
- Bally, J., Devine, D. & Alten, V. 1996, *ApJ*, 473, 921
- Bally, J., Devine, D., Alten, V. & Sutherland, R. 1997, *ApJ*, 478, 603
- Bally, J., Devine, D. & Reipurth, B. 1996, *ApJ*, 473, 49
- Bally, J. & Lada, C. J. 1983, *ApJ*, 265, 824
- Bally, J., Langer, W. D., Stark, A. A., & Pound, M. in “*I.A.U. Colloquium No. 147: Fragmentation in Molecular Clouds and Star Formation*”, ed. E. Falgarone & J. L. Puget
- Bally, J., Langer, W. D., Stark, A. A. & Wilson R. W. 1987, *ApJL*, 313, L45
- Bally, J., Wilson, R. W., Langer, W. D., Stark, A. A., & Pound, M. W. 1989, in “*I.A.U. Colloquium No. 120: Structure and Dynamics of the Interstellar Medium*”, ed. Tenorio-Tagle
- Billawala, Y., Bally, J. & Sutherland, R. 1997, in preparation
- Blaauw, A. 1991, in *Astrophysical Jets*, eds. C. J. Lada & N. D. Kylafis (Dordrecht : Kluwer), p.125

- Cêrnis, K. 1990, *Astrophysics and Space Science*, 166, 315
- Crutcher, R. M., Troland, T. H., Goodman, A. A., Heiles, C., Kazès, I. & Myers, P. C. 1993, *ApJ*, 407, 175
- Crutcher, R. M., Troland, T. H., Lazareff, B. & Kazès, I. 1996, *ApJ*, 456, 217
- Elmegreen, B. G. 1985, *ApJ*, 299, 196
- Elmegreen, B. G. 1997, *ApJ*, 477, 196
- Falgarone, E. 1992, *Proc. IAU Symp. 150, Astrochemistry of Cosmic Phenomena*, ed. P. D. Singh (Kluwer : Dordrecht), p.159
- Falgarone, E. & Phillips, T. G. 1991, *Proc. IAU Symp. 147, Fragmentation of Molecular Clouds and Star Formation*, eds. E. Falgarone, F. Boulanger & G. Duvert (Kluwer : Dordrecht), p.119
- Falgarone, E., Phillips, T. G. & Walker, C., K. 1991, *ApJ*, 378, 186
- Falgarone, E. & Puget, J. L. 1986, *A&A*, 162, 235
- Ferrini, F., Marchesoni, F. & Vulpiani, A. 1983, *MNRAS*, 202, 1071
- Fleck, R. C. 1988, *ApJ*, 328, 299
- Fleck, R. C. 1996, *ApJ*, 458, 739
- Goodman, A. A., Crutcher, R. M., Heiles, C., Meyers, P. C. & Troland, T. H. 1989, *ApJ*, 338, L61
- Heiles, C. 1984, *ApJS*, 55, 585
- Henriksen, R. N. & Turner, B. E. 1984, *ApJ*, 287, 200
- Herbig, G. H. & Jones, B. F. 1983, *AJ*, 88, 1040
- Hodapp, K.-W. & Ladd, E. F. 1995, *ApJ*, 453, 715
- Juvela, M. 1997, *A&A*, 322, 943
- Knee, L. B. G. & Sandell, G. 1997, preprint
- Lada, C. J., Alves J. & Lada, E. A. 1996, *AJ*, 111, 1964
- Lada, C. J. & Lada, E. A. 1995, *AJ*, 109, 1682
- Lada, C. J., Lada, E. A., Clemens, D. P. & Bally, J. 1994, *ApJ*, 429, 694.
- Lada, E. A., Strom, K. M. & Myers, P. C. 1993, in *Protostars and Planets III*, eds. E. H. Levy & J. I. Lunine (Arizona : University of Arizona Press), p.245
- Langer, W. D., Wilson, R. W., Goldsmith, P. F. & Beichman, C. A. 1989, *ApJ*, 337, 355
- Larson, R. B. 1981, *MNRAS*, 194, 809
- Larson, R. B. 1995, *MNRAS*, 272, 213
- Lord, S. D., Malhotra, S., Lim, T., Helou, G., Rubin, R. H., Stacey, G. J., Hollenbach, D. J., Werner, M. W., Thronson, H. A., JR, Beichman, C. A., Dinerstein, H., Hunter, D. A., Lo, K. Y. & Lu, N. Y. 1996, *A&A*, 315, 117
- McKee, C. F. & Zweibel, E. G. 1995, *ApJ*, 440, 686
- Mestel, L. 1965, *Q. Jl. RAS*, 6, 161, 265
- Miesch, M. S. & Bally, J. 1994, *ApJ*, 429, 645
- Mouschovias, T. Ch. 1976a, *ApJ*, 206, 753
- Mouschovias, T. Ch. 1976b, *ApJ*, 207, 141
- Padoan, P., Jones, B. J. T. & Nordlund, Å. 1997, *ApJ*, 474, 730
- Padoan, P., Juvela, M., Bally, J. & Nordlund, Å. 1997, *ApJ*, submitted
- Padoan, P. & Nordlund, Å. 1997, *ApJ*, submitted
- Padoan, P., Nordlund, Å. & Jones, B. J. T. 1997, *MNRAS*, in press
- Parker, D. A. 1973, *MNRAS*, 163, 41
- Sandell, G., Knee, L. B. G., Aspin, C., Robson, I. E., Russell, A. P. G. 1994, *A&A*, 285, 1
- Scalo, J. M. 1987, in *Interstellar Processes*, ed. D. J. Hollenbach & H. A. Thronson (Reidel), p. 349
- Scalo, J. 1990, in *Physical Processes in Fragmentation and Star Formation*, eds. R. Capuzzo-Dolcetta, C. Chiosi & A. Di Fazio, (Kluwer : Dordrecht), p.151
- Strittmatter, P. A. 1966, *MNRAS*, 132, 359
- Strom, S. E., Grasdalen, G. & Strom, K. M., 1974, *ApJ*, 191, 111
- Strom, K. M., Margulis & M., Strom, S. E. 1989, *ApJ*, 345, 79

Strom, K. M., Newton, G., Strom, S. E., Seaman, R. L., Carrasco, L., Cruz-Gonzalez, I., Serrano, A., Grasdalen, G. L. 1989, ApJS, 71, 183

Whitworth, A. 1979, MNRAS, 186, 59

Wright, E. L., Mather, J. C., Bennett, C. L., Cheng, E. S., Shafer, R. A., Fixsen, D. J., Eplee, R. E., JR., Isaacman, R. B., Read, S. M., Boggess, N. W., Gulkis, S., Hauser, M. G., Janssen, M., Kelsall, T., Lubin, P. M., Meyer, S. S., Moseley, S. H., JR., Murdock, T. L., Silverberg, R. F., Smoot, G. F., Weiss, R. & Wilkinson, D. T. 1991, ApJ, 381, 200

Zweibel, E. G. & Josafatsson, K. 1983, ApJ, 270, 511

Figure and Table captions:

Figure 1: Integrated antenna temperature of $J=1\rightarrow 0$ ^{13}CO for velocities 0 to 15 km s^{-1}

Figure 2: Integrated antenna temperature of the L1448 (left panel), B 5 (center panel), and the 5 pc model (right panel). As the real data, the synthetic image shows filamentary structure, cores, and partial shells.

Figure 3: Mean spectra of L1448 (upper panel), B5 (middle panel), and the entire Perseus molecular cloud (lower panel). The dashed curves shows the mean spectrum of the model. Each spectrum is centered around its own mean.

Figure 4: Probability distribution of velocity integrated antenna temperature for the three clouds as in figure 3. The dashed curve shows the theoretical distribution.

Figure 5: A $30' \times 30'$ map of individual $J=1\rightarrow 0$ ^{13}CO spectra around the brightest region of L1448. The velocity interval for each spectrum shown is 6.5 km s^{-1} (the actual interval used for the statistical analysis was 15 km s^{-1}) and the antenna temperature ranges from 0 to 6 K.

Figure 6: As in figure 5 but for the B5 cloud.

Figure 7: As in figure 5 but for the 5 pc model cloud.

Figure 8: Histograms of the first four statistical moments of the spectra of the entire observed region of Perseus. Upper left: distribution of centroid velocities. Upper right: distribution of velocity dispersions (line widths). Lower left: distribution of skewness. Lower right: distribution of kurtosis. Vertical dashed lines show the values of the same statistical moments for the mean spectrum.

Figure 9: As in figure 8 but for L1448.

Figure 10: As in figure 8 but for B5.

Figure 11: As in figure 8 but for the 5 pc model

cloud.

Figure 12: Scatter plots of equivalent width versus velocity integrated antenna temperature for the three observed regions (three upper panels) and for the 5 pc model cloud (lower panel). The diamond symbols show the mean value of the equivalent width in each interval of integrated antenna temperature and the "error bars" show the one σ distribution around the mean. Intervals of integrated antenna temperature were chosen to contain the same number of points.

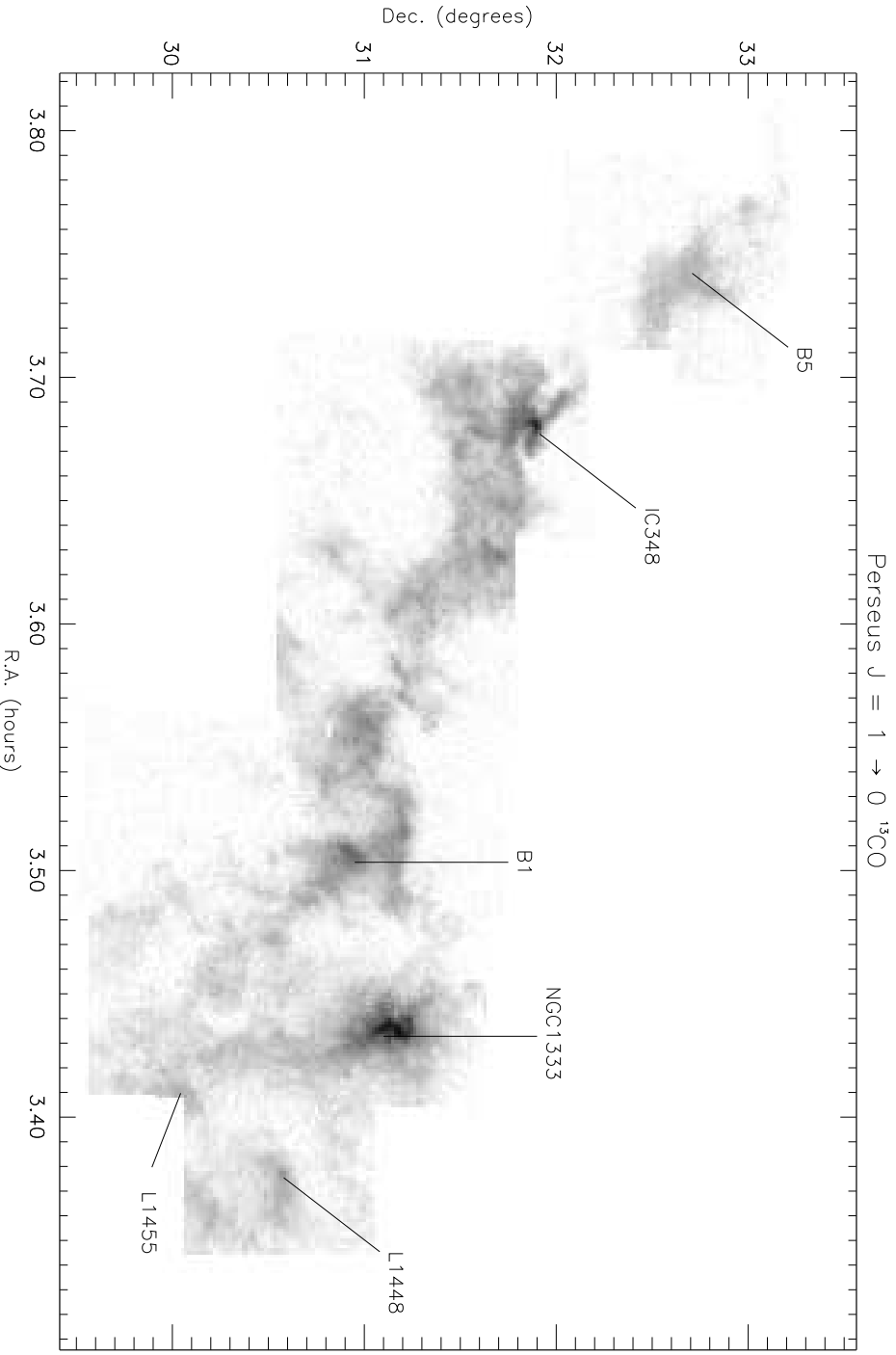


Fig. 1. —

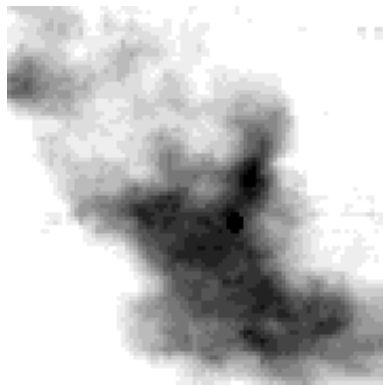


Fig. 2.—

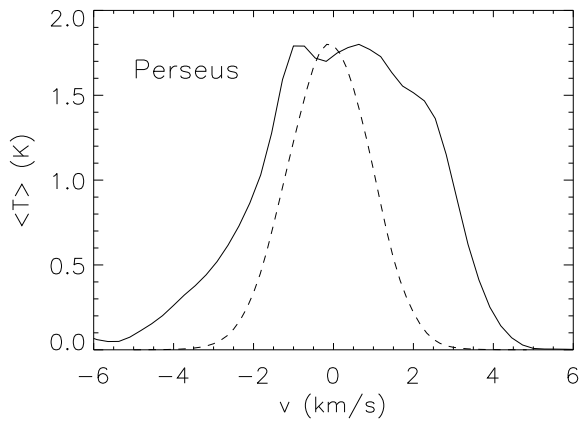
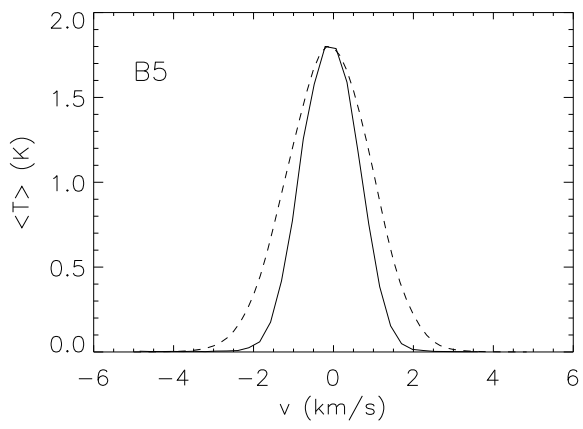
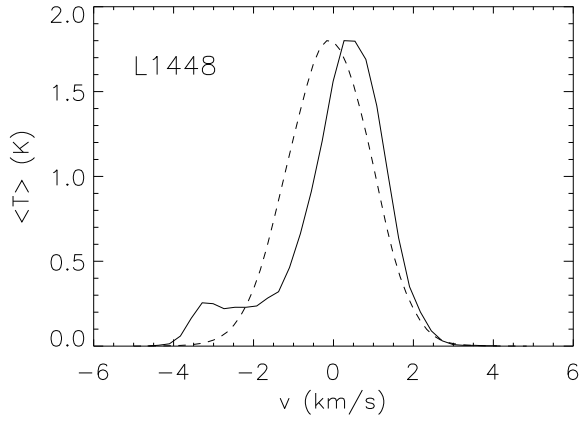


Fig. 3.—

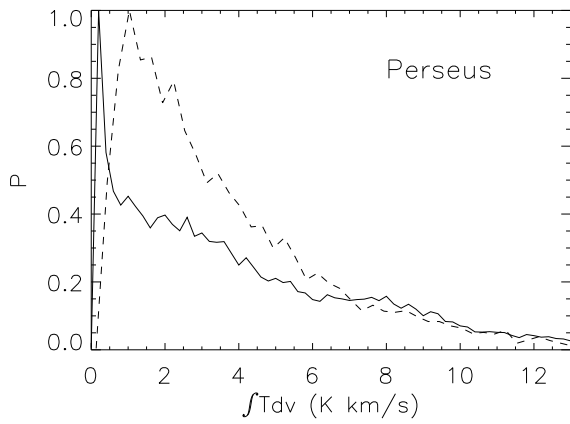
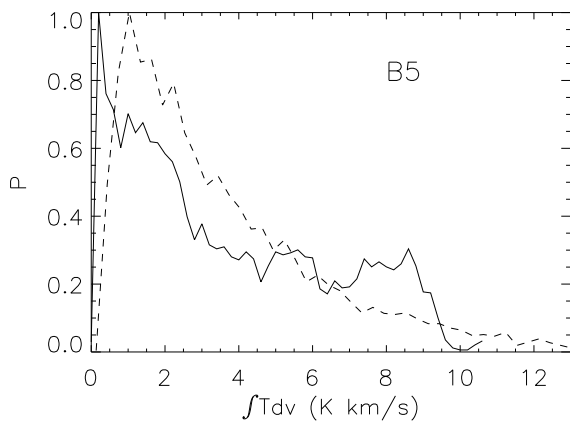
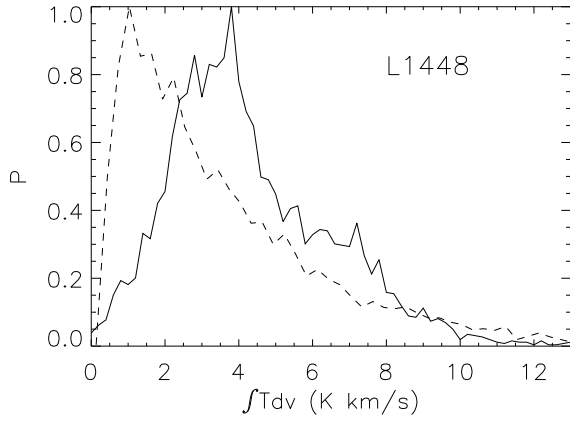


Fig. 4.—

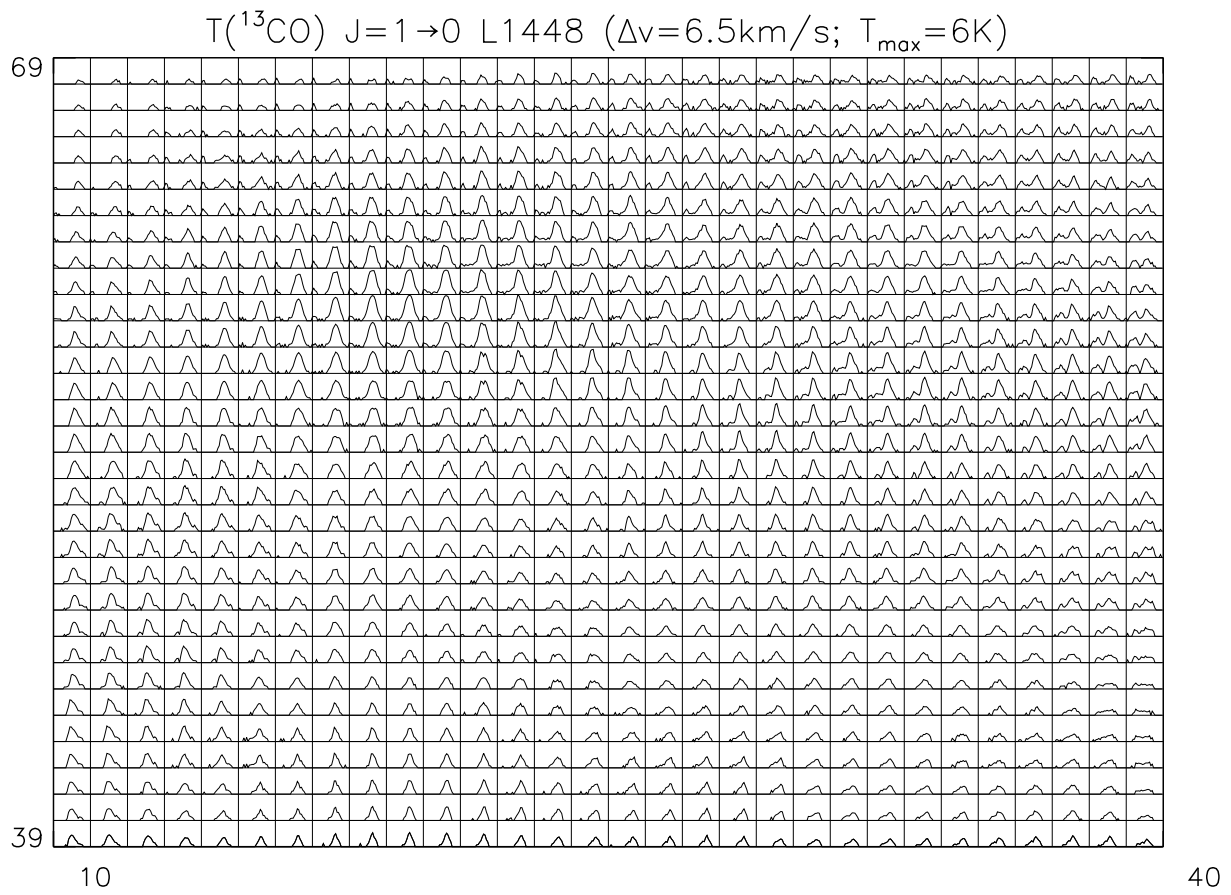


Fig. 5.—

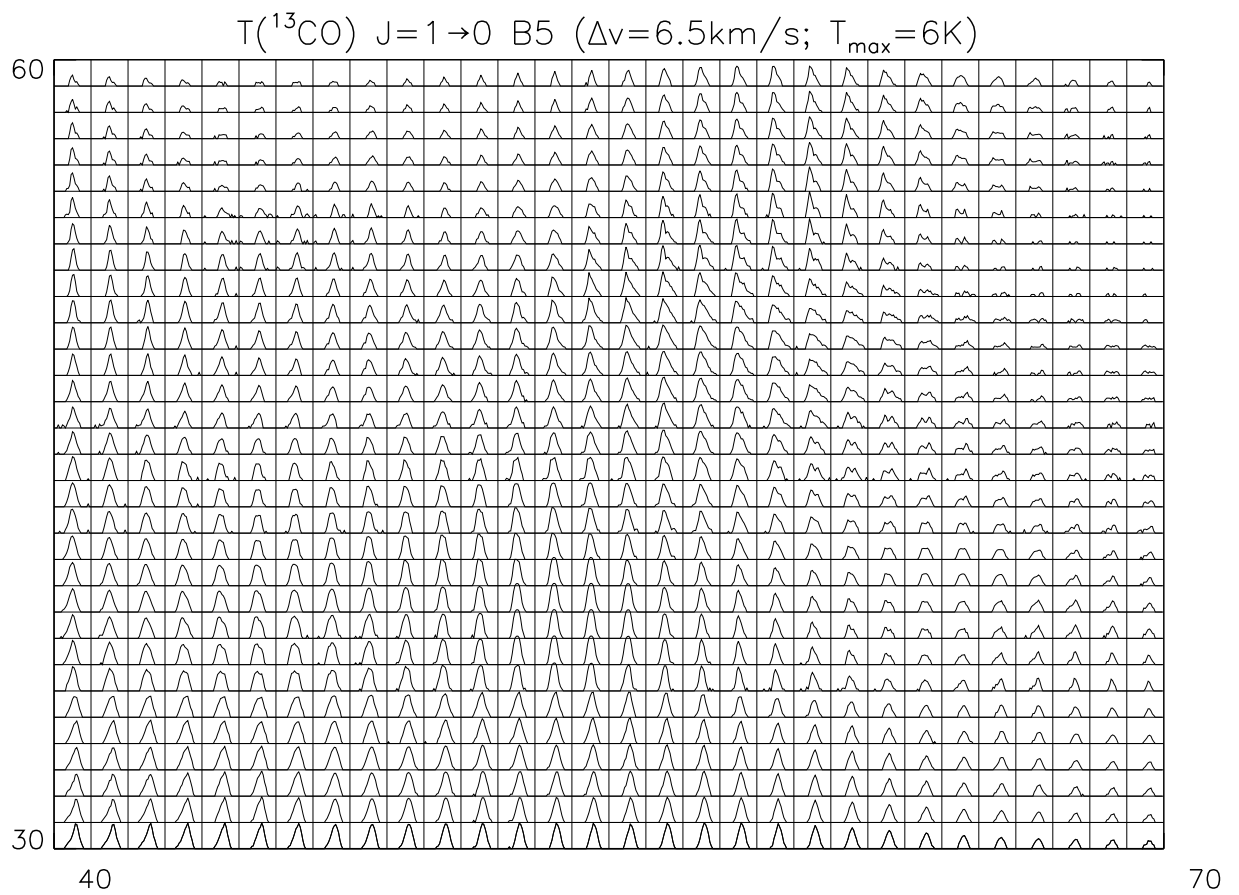


Fig. 6.—

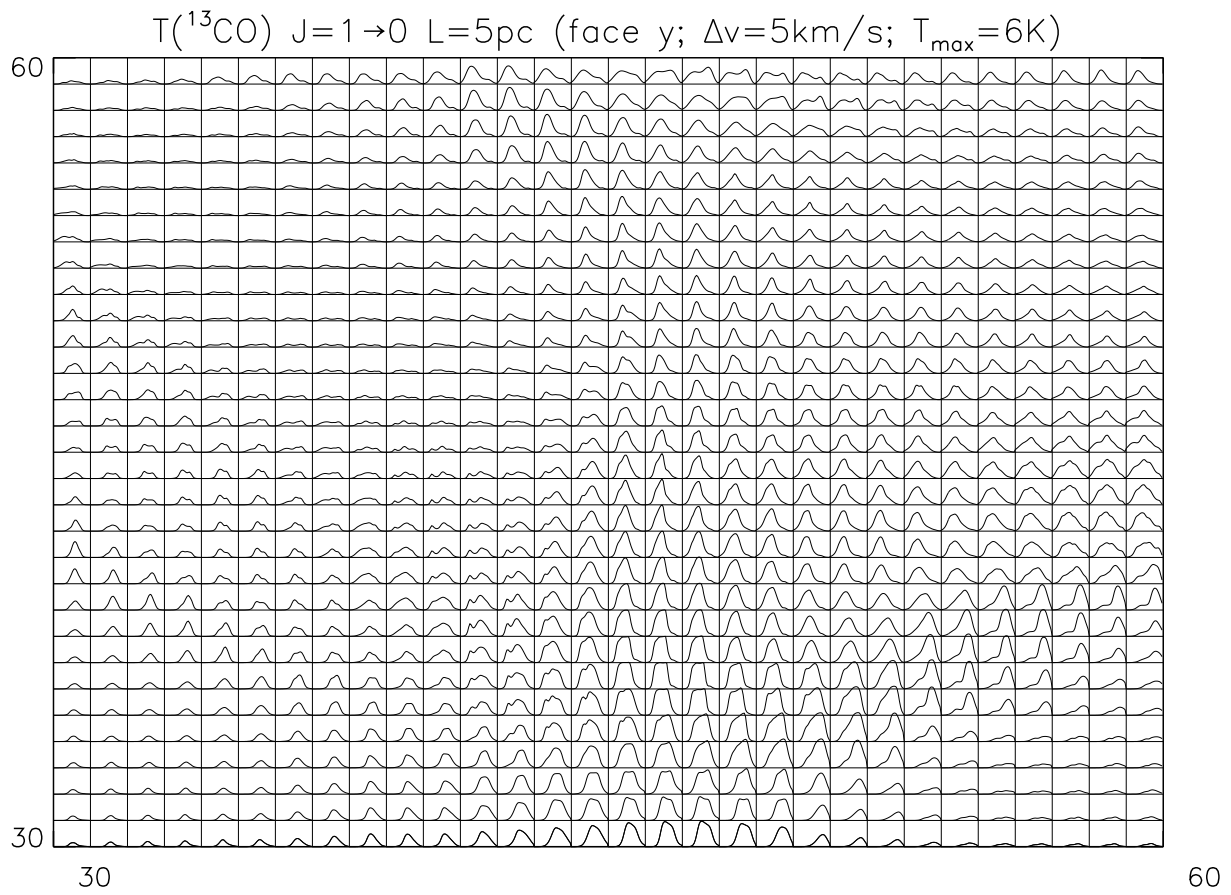


Fig. 7.—

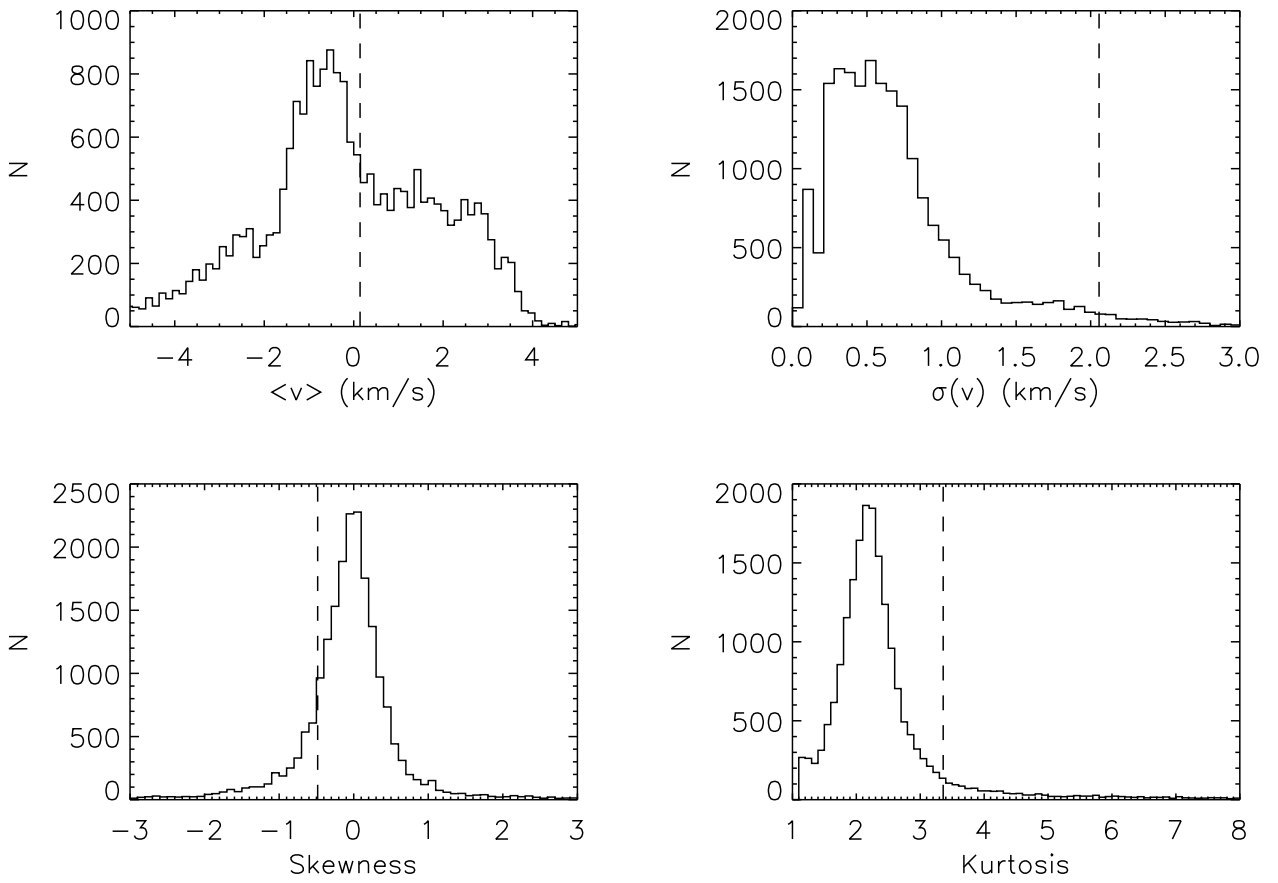


Fig. 8.—

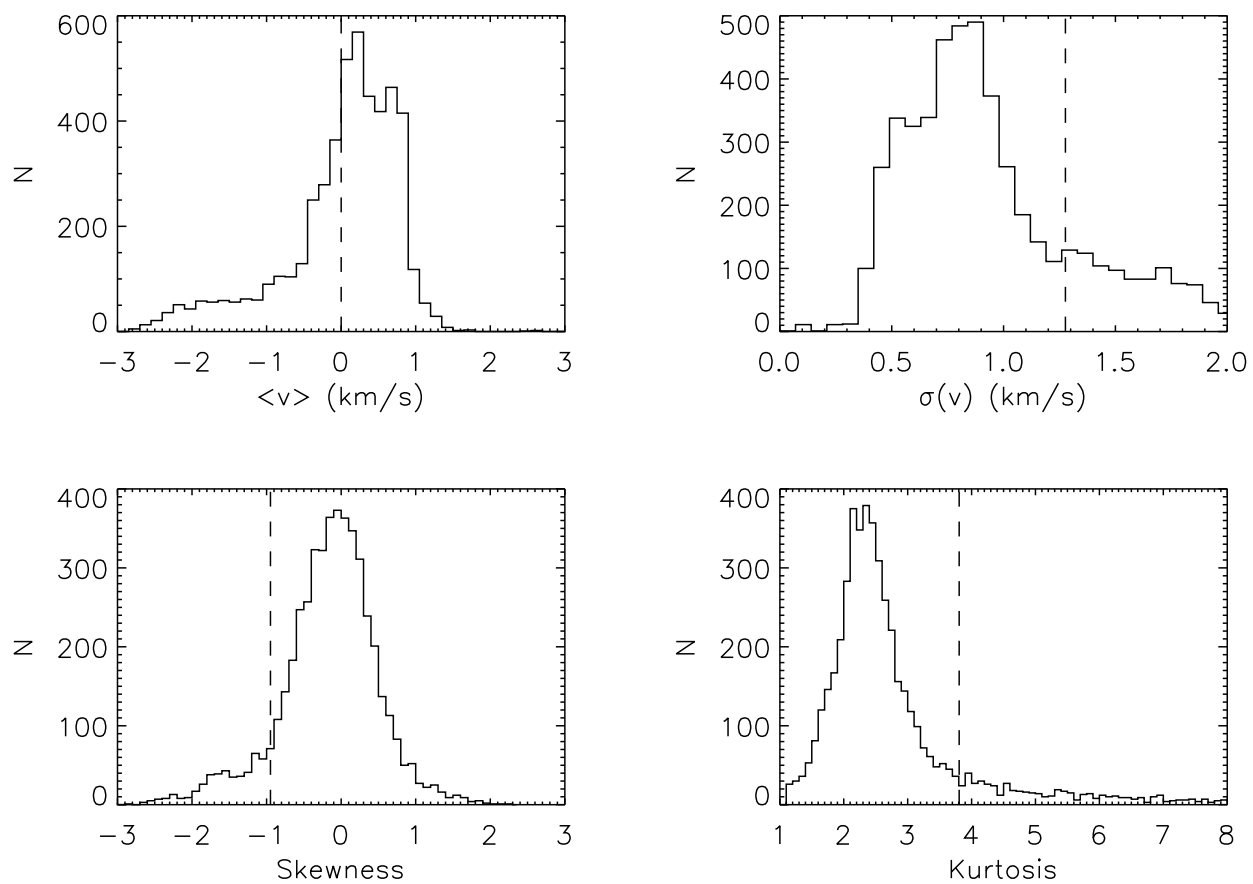


Fig. 9.—

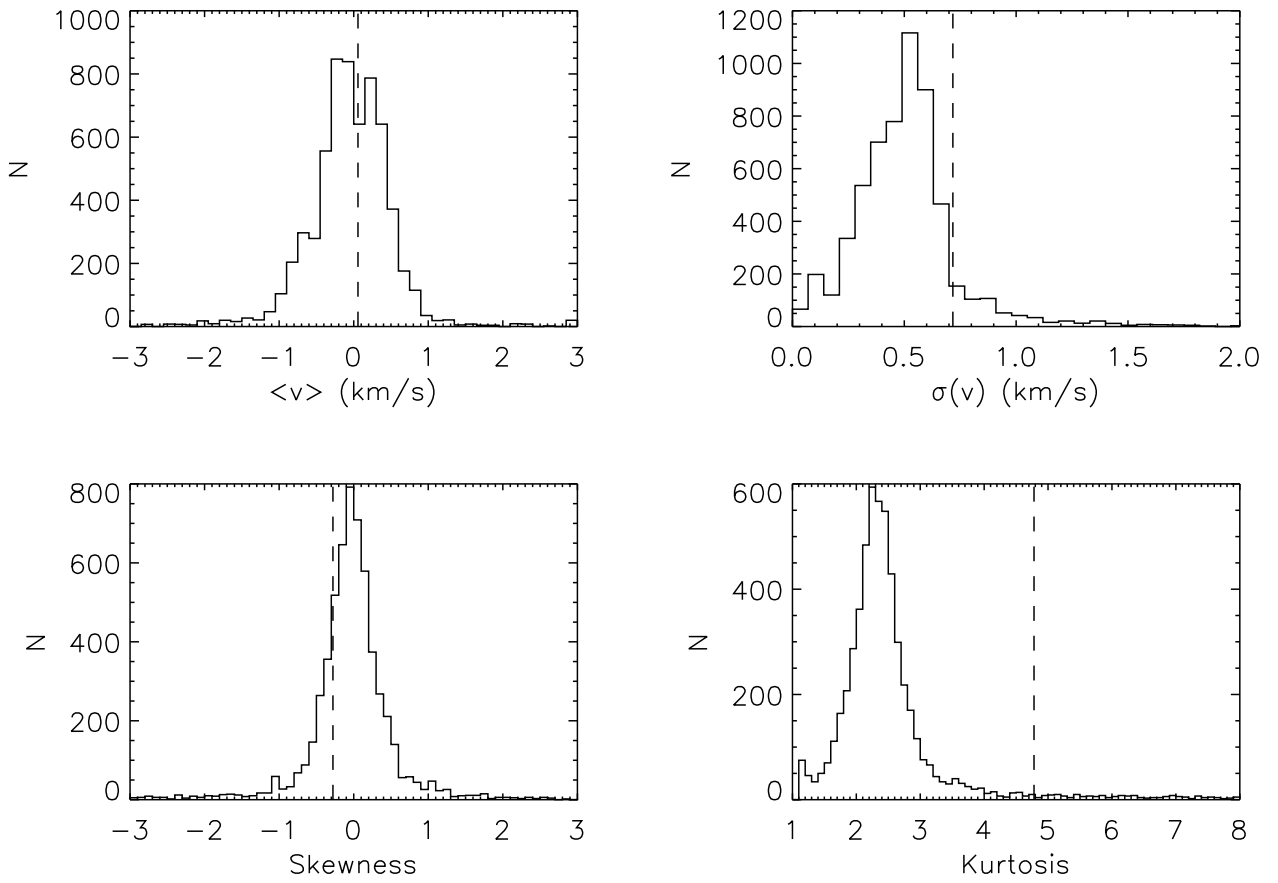


Fig. 10.— As in figure 8 but for B5.

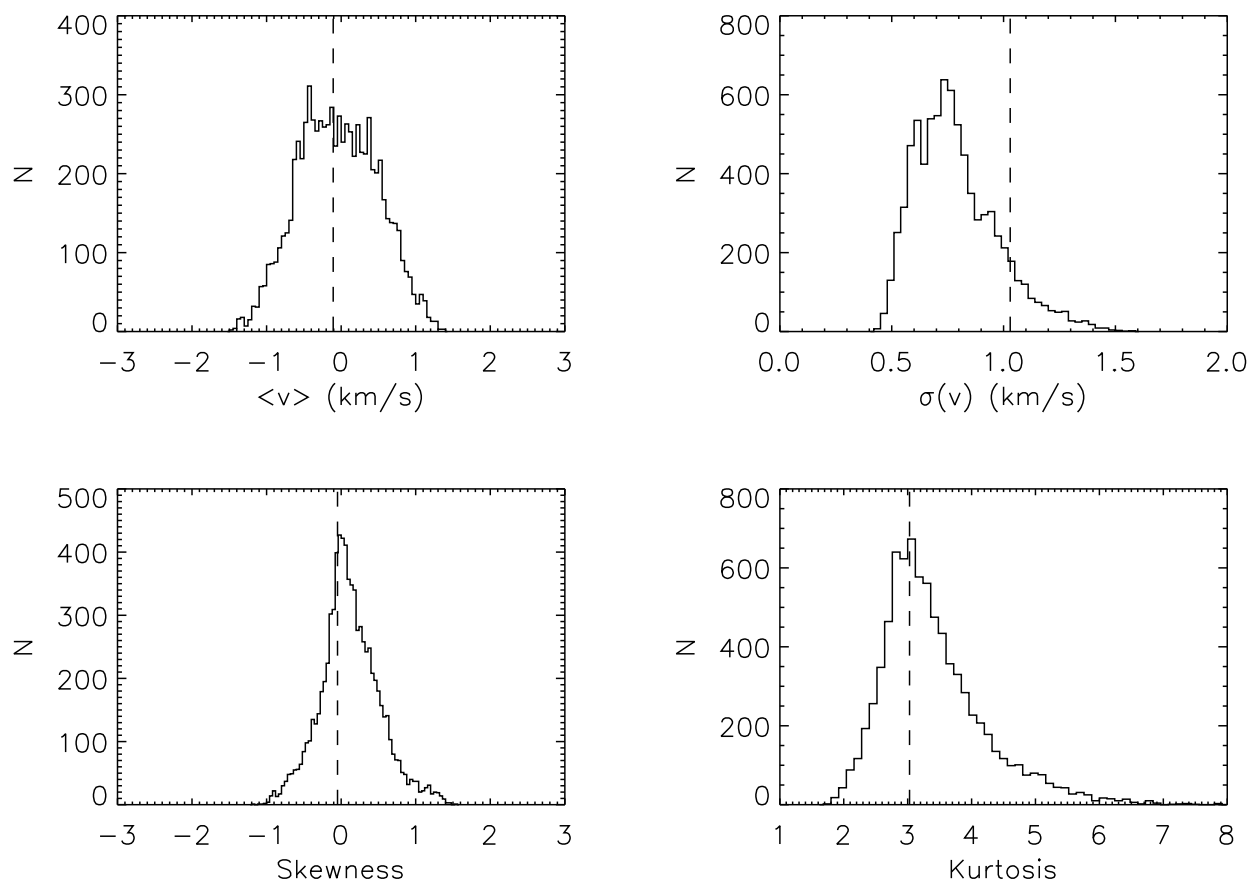


Fig. 11.—

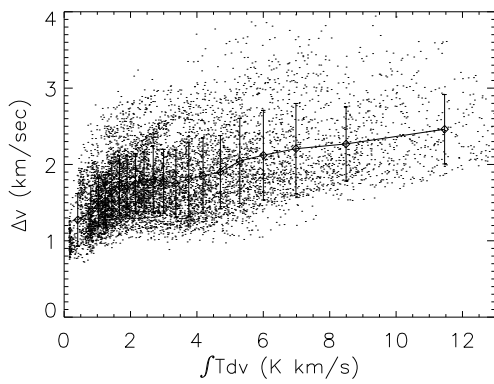
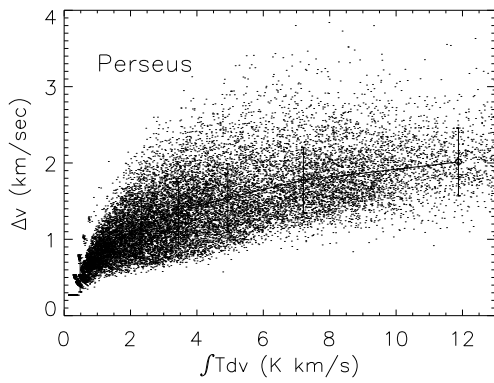
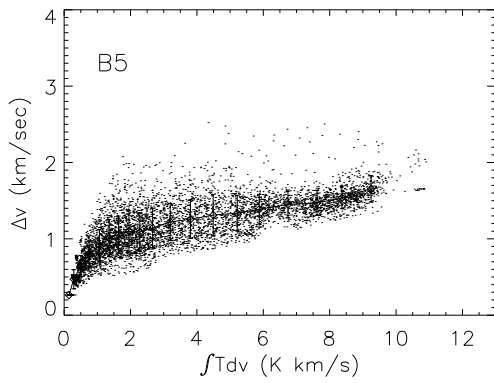
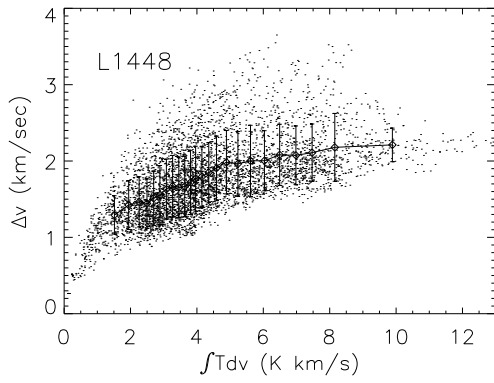


Fig. 12.—